DOI: 10.1002/ejic.200601180

Lanthanide Complexes with a Calix[8]arene Bearing Phosphinoyl Pendant Arms

Lada N. Puntus,[a,b] Anne-Sophie Chauvin,[a] Sabi Varbanov,[a,c] and Jean-Claude G. Bünzli*[a]

Keywords: Lanthanides / Calixarenes / Europium / Luminescence

The phosphinoyl-substituted macrocyclic receptor B_8bL^8, derived from *p-tert*-butylcalix[8]arene, was synthesized and its structure was studied in solution. According to temperature-dependent ^1H and ^{31}P NMR spectroscopic data, the calix[8]arene adopts a so-called *in–out* cone conformation. To investigate the influence of the narrow rim substitution, interaction with trivalent lanthanide ions, Ln^{III} (Ln = La, Eu, Tb, Lu), was probed by MS, UV/Vis and NMR spectroscopic titrations. Although both 1:1 (in the presence of triflate) and 2:1 (in the presence of nitrate) $Ln:B_8bL^8$ complexes could be isolated in the solid state, the major species present in methanol is the 1:1 complex, irrespective of the anion. NMR spectroscopic data point to a common conformation for the 1:1 complexes in solution, the lanthanide ions being coordinated by four of the eight phosphinoyl arms, with a coordination sphere completed by methanol molecules or by nitrate ions, as ascertained by IR and MS spectra. The ligand displays a weak absorption at 360 nm that can be assigned to an intraligand charge-transfer (ILCT) state, which is very sensitive to coordination. Photophysical data of the Eu^{III} 2:1 complex point to both metal ion sites providing a very similar chemical environment for the lanthanide ions, with no coordinated water, which is contrary to what is observed for the 1:1 complex. The use of optical electronegativity to predict the energy of the charge-transfer states in the lanthanide systems with inequivalent ligands is discussed and extensive analysis of the vibronic satellites of the $Eu(^5D_0 \rightarrow {}^7F_J)$ transitions ascertains conclusions drawn on the Eu^{III} coordination.

Introduction

Calix[*n*]arenes, or [1$_n$]metacyclophanes, present excellent coordination[1] and extraction[2–4] capabilities, in addition to being adequate platforms for the design of catalysts[5] or optical sensors.[6] They also provide suitable frameworks for the construction of more complex noncovalent structures.[7–9] Central to these applications are (1) the availability of calixarenes in various ring sizes, up to $n = 20$,[10] (2) their capacity to assume different conformations that can be tuned by the nature of the substituents and/or by two- or four-point intramolecular bridging,[11] which leads to controlled luminescent properties[12] and (3) their easy functionalization both at the wide and narrow rims, a versatility that opens perspectives in many fields of chemistry. Our interest in lanthanide complexes with calixarenes lies in the development of bimetallic model molecules for the study of energy transfer processes and magnetic interactions,[13] as well as in the design of lanthanide/actinide extraction systems and luminescent probes. With respect to the latter goals, we, among others, have been focusing on *p-tert*-butylcalix[*n*]arenes fitted with dimethylphosphinoylmethylene pendant groups on the narrow rim (Scheme 1) because the latter are known to be good complexation groups for trivalent lanthanide ions, Ln^{III}. In addition, similar hosts bearing diphenylphosphinoylmethylene arms have been previously proposed.[14–16] The smaller macrocyclic receptor derived from calix[4]arene, B_4bL^4, adopts a flattened cone conformation. It reacts with lanthanide ions to yield both 1:1 and 1:2 (Ln/L) stable complexes with Ln^{III} ions in acetonitrile; the solvent composition, particularly its water content, influences strongly the solvation state of the macrocyclic edifices as well as their luminescent properties.[17] This macrocycle is also quite convenient for the binding of 3d metal ions.[18] When the number of phenolic units is increased to six to yield B_6bL^6, the resulting macrocycle exists as a mixture of conformers in dmso with a time-averaged alternate *in–out* conformation at elevated temperature (405 K) of C_{6v} symmetry. Because of the larger conformational flexibility, both 1:1 and 1:2 complexes with Ln^{III} ions are less stable than the corresponding ones with the

[a] École Polytechnique Fédérale, Lausanne, Laboratory of Lanthanide Supramolecular Chemistry, BCH 1401, 1015 Lausanne, Switzerland
E-mail: anne-sophie.chauvin@epfl.ch
jean-claude.bunzli@epfl.ch
[b] Russian Academy of Sciences, Institute of Radio Engineering & Electronics, 125009 Moscow, Russia
E-mail: lada_puntus@mail.ru
[c] Bulgarian Academy of Sciences, Institute of Polymers, 1113 Sofia, Bulgaria
E-mail: varbanov@orgchm.bas.bg
Supporting information for this article is available on the WWW under http://www.eurjic.org or from the author.

analogous calix[4]arene, but these complexes still display interesting photophysical properties.[19] Liquid–liquid extraction studies have demonstrated the separation ability of B_4bL^4 and B_6bL^6 for the lighter actinides, as compared to Ln^{III} ions, and the calix[6]arene receptor revealed to be the best extractant.[20] Owing to the large dimension of their annulus, calix[8]arenes are promising receptors both for medium-sized organic compounds[21] and large metal cations; for instance, they can encapsulate up to two Ln^{III} ions in the same molecular edifice.[13,22] For *p*-substituted calix[8]-arenes, the 1:1 versus 2:1 stoichiometry is simply tuned by the strength of the base used to deprotonate the hydroxy groups.[23,24] However, most of the reported complexes have 2:1 stoichiometry,[25,26] whereas 1:2 molecular ratios are less common.[27] The purpose of this paper is to investigate the influence of the narrow rim substitution of *p*-*tert*-butylcalix[8]arene by phosphinoyl groups on the coordination and photophysical properties of both the octamer toward trivalent lanthanide ions and the resulting complexes. In addition, we probe the effect of the coordination strength of the anion with regard to both the stoichiometry of the complexes and the coordination mode of the macrocycle.

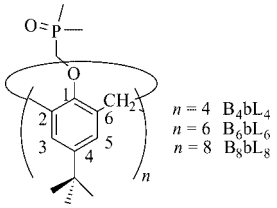

Scheme 1.

Results and Discussion

Synthesis and Structural Characterisation of Calixarene B_8bL^8 in Solution

The macrocyclic receptor B_8bL^8 (Scheme 1) was prepared in 46% yield by a Williamson reaction by refluxing the octasodium derivative of *p*-*tert*-butylcalix[8]arene and chloro(dimethylphosphinoyl)methane in xylene (Scheme 2).

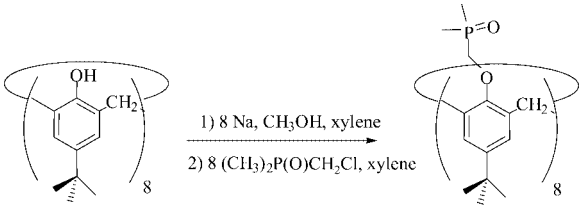

Scheme 2.

The structure of B_8bL^8 in a 3.4×10^{-3} M [D_4]methanol solution was established by temperature-dependent NMR spectroscopy. At 293 K, the $^{31}P\{^1H\}$ NMR spectrum displays a singlet at δ = 44.8 ppm, which indicates that the eight phosphorus atoms are equivalent. ^1H NMR spectroscopic signals for all protons appear as singlets (Figure 1), except for the $CH_2(P{=}O)$ and $CH_3(P{=}O)$ groups, which generate doublets owing to the coupling with the ^{31}P atom.[19,28,29] All ^1H and ^{13}C NMR spectroscopic data are consistent with a cone conformation,[14,30–32] which suggests a time-averaged molecular structure resulting from fast interconversion between the different conformers. At 213 K, the ^1H NMR spectrum is less well-resolved with moderately broadened signals owing to higher solvent viscosity (Figure 1). A double quantum filtered correlation spectroscopic (DQF-COSY) experiment points again to only one conformation for the isomers: the observed correlation peaks can be assigned to (1) CH_3 groups bound to the same carbon atom (δ = 1.36 and 0.82 ppm), (2) aromatic protons belonging to one phenol ring (δ = 7.36 and 6.56 ppm) and (3) protons from the AB spin system of the eight bridging methylene groups (δ = 4.3 and 3.9 ppm). Appearance of a correlation peak between the CH_2 and $CH_3P{=}O$ groups (see Figure 2) in the rotating frame Overhauser enhancement spectroscopic experiment (ROESY) could be the result of partial inversion, which results from *p*-*tert*-butyl moieties that swing through the annulus. Indeed, two dynamic processes were detected in large calixarenes with substituted phenol groups: macrocyclic ring interconversion and pinched conformer interconversion. The former takes place by way of two different mechanisms: *tert*-butyl-through-the-annulus and oxygen-through-the-annulus pathways,[8,33] The first mechanism, in which the aryl groups swing through the annulus in sequence, always operates in unbridged large calixarenes, as demonstrated for *p*-*tert*-butylcalix[6]arenes.[30,34,35] Alternatively, the presence of sufficiently bulky groups at the narrow rim, as it is the case for B_8bL^8, inhibits oxygen-through-the-annulus interconversion so that ring interconversion can only proceed by the *tert*-butyl-through-the-annulus route.

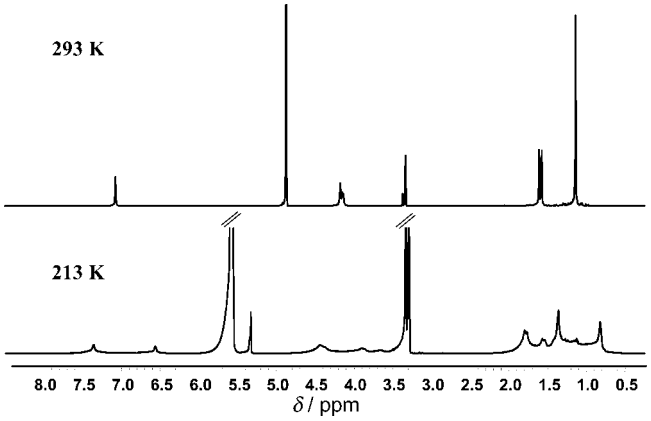

Figure 1. ^1H NMR spectra of the 3.4×10^{-3} M solution of B_8bL^8 in CD_3OD at (a) 293 and (b) 213 K.

^1H and ^{31}P NMR spectroscopic data were obtained over a wide temperature range (193–353 K; Figure S1, Supporting Information). At the lowest temperature, the conformational interconversion processes are not yet completely frozen despite the observation of two distinct resonances in the ^{31}P spectrum. For $T \geq 293$ K, sharp, well-resolved reso-

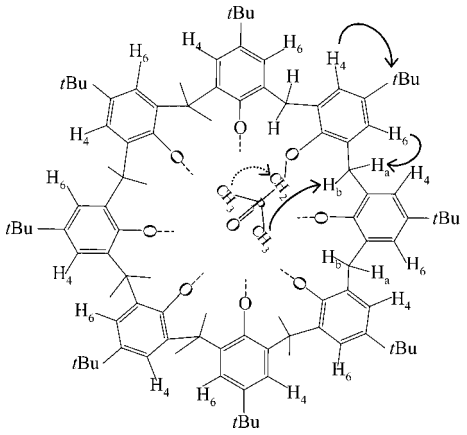

Figure 2. ROESY contacts observed at 213 K for B_8bL^8 in CD_3OD: plain arrows are for the ligand alone and dotted arrows for the solution containing one equivalent of $Lu(Otf)_3$.

nances are recorded in both the ^1H and ^{31}P NMR spectra. This reveals that the activation barrier for macrocyclic ring interconversion is low.

Interaction of B_8bL^8 with Ln^{III} in Methanol

To obtain information on the interaction between B_8bL^8 and lanthanide ions, a $8.1–8.6 \times 10^{-4}$ M solution of the macrocycle in MeOH was titrated with $Ln(OTf)_3 \cdot xH_2O$ (Ln = La, Eu, Lu; typically 10^{-4} M, $x = 10$ for La, 7 for Eu and 9 for Lu) and $Ln(NO_3)_3 \cdot xH_2O$ (Ln = La, Eu; typically 10^{-3} M, $x = 4$ for Eu and 3 for Lu) up to a ratio of $R = [Ln^{III}]_{tot}/[B_8bL^8]_{tot} = 4.5$. Titrations were first monitored by electrospray mass spectrometry (ESMS, see Tables S1 and S2, Supporting Information). For $R \leq 1$, both 1:2 $[Eu(B_8bL^8)_2]^{3+}$ (m/z = 1396.40, calcd. 1396.22) and 1:1 $[Eu(B_8bL^8)(CH_3COOH)]^{3+}$ (m/z = 743.32, calcd. 743.45) species are observed. An increase in R leads to the disappearance of the 1:2 species. When R reaches 2, the main species is $[Eu(B_8bL^8)(Otf)]^{2+}$ (m/z = 1159.24, calcd. 1158.95), but $[Eu(B_8bL^8)]^{3+}$ (m/z = 723.20, calcd. 723.44) is also observed. No signal from the free ligand is detected in the latter case, which points to the formation of a stable 1:1 species. Titration of the macrocycle solution with $Eu(NO_3)_3 \cdot 4H_2O$ shows a similar behaviour, except for the stronger coordination of the counterions, as demonstrated by the presence of $[Eu(B_8bL^8)(NO_3)]^{2+}$ (m/z = 1114.97, calcd. 1115.49), $[Eu(B_8bL^8)(NO_3)(H_2O)_2]^{2+}$ (m/z = 1133.44, calcd. 1134.16) and $[Eu(B_8bL^8)(NO_3)(CH_3COOH)]^{2+}$ (m/z = 1145.47, calcd. 1145.52) species for $R = 1$ (Table S2, Supporting Information). Formation of species with stoichiometric ratio Eu/B_8bL^8 of 2:1 was not detected in this case, probably owing to its low solubility; a precipitate starts to appear when $R > 1$.

The titrations were repeated with UV/Vis monitoring, starting from concentrations of 1.1×10^{-4} M for B_8bL^8 and adding lanthanide triflates with concentrations of $\approx 8 \times 10^{-3}$ M. Plots of absorbance versus R evidenced at least two complexed species (Figure S2, Supporting Information) and factor analysis revealed four absorbing species (B_8bL^8, 1:2, 1:1, 2:1), which could be satisfactorily fitted to the following model (Table 1):

$Ln^{3+} + B_8bL^8 \rightarrow [Ln(B_8bL^8)]^{3+}$ $\log K_{11}$

$Ln^{3+} + 2\ B_8bL^8 \rightarrow [Ln(B_8bL^8)_2]^{3+}$ $\log K_{12}$

$2\ Ln^{3+} + B_8bL^8 \rightarrow [Ln_2(B_8bL^8)]^{6+}$ $\log K_{21}$

Table 1. Log K_{ij} values ($\pm$ 0.2) extracted from the titration of B_8bL^8 with lanthanide triflates in methanol, at 293 K.

Ln	$\log K_{12}$	$\log K_{11}$	$\log K_{21}$
La	4.4	6.9	4.9
Eu	4.3	7.2	5.0
Lu	5.6	7.4	4.9

Because the UV/Vis spectra of the complexes are heavily correlated, these data should be taken as a first estimate. The stability constants obtained are smaller than the ones reported for B_4bL^4[17] and B_6bL^6[19] as a consequence of the smaller degree of preorganisation of the octamer. The K_{11} values are about two orders of magnitude larger than the K_{12} and K_{21} constants. Calculation of the speciation of Eu^{III} with these data and a total ligand concentration between 10^{-4} and 10^{-3} M shows that for $R = 1$, the 1:1 species is always largely predominant (> 93%). For all the concentrations at which the titrations have been conducted, and for R in the range 0.5–2.0, the concentration of the bimetallic 2:1 complex remains extremely small.

Finally, the speciation was confirmed by ^1H and $^{31}P\{^1H\}$ NMR spectroscopic titration at 293 K. The free ligand, 1:2 and 1:1 species coexist in 3.3×10^{-3} M methanolic solutions of B_8bL^8 that contain lutetium triflate when $R < 1$ (Figure 3). For $1 < R < 1.6$, the minor 1:2 species disappears whereas the 1:1 species grows until $R > 1.6$. Together with ESMS and spectrophotometric titration data, this can be interpreted as the formation of a thermodynamically stable complex with 1:1 stoichiometry. Coordination through the phosphinoyl groups is established as both the ^1H and

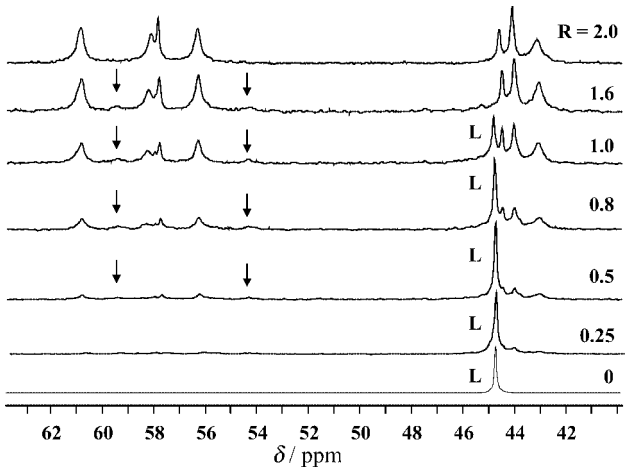

Figure 3. Titration of a B_8bL^8 solution (3.3×10^{-3} M) by $Lu(OTf)_3 \cdot 9H_2O$ (4.5×10^{-2} M) in CD_3OD as monitored by $^{31}P\{^1H\}$ NMR spectroscopy at 293 K, $R = [Lu^{III}]_t/[B_8bL^8]_t$; arrows point to the signal of the minor 1:2 species, while L denotes the free ligand signals.

$^{31}P\{^1H\}$ NMR signals from the phosphinoyl arms are affected by the complexation. Two ^{31}P signals are observed, shifted from 44.6 ppm for the free ligand to 43.7 ppm ($\Delta\delta$ = 0.9 ppm) and 58.5 ppm ($\Delta\delta$ = 13.8 ppm) for the 1:1 lutetium complex. This points to two different chemical environments for the phosphorus atoms in a 1:1 ratio, which suggests that the octamer has four coordinated and four uncoordinated arms. This was further ascertained by temperature-dependent 1D and 2D NMR experiments described in the next section. Taking into account all the results obtained during the titrations, one can conclude that the ESMS, UV/Vis and NMR spectroscopic data are consistent and point to the predominance of the 1:1 species.

Solution Structure of the 1:1 Complexes with $Lu(OTf)_3$ and $Lu(NO_3)_3$

The ^1H NMR spectrum of a B_8bL^8 solution 3.3×10^{-3} M in [D_4]methanol containing one equivalent of lutetium triflate (Figure 4) displays three typical groups of resonances at 213 K: (1) four signals between 6.6 and 7.6 ppm from the 16 aromatic protons, (2) three pairs of doublets in the range 3.8 to 4.7 ppm from the eight bridging methylene groups and two signals from eight (CH_2)P=O groups, and (3) two groups of signals between 0.8 and 1.5 ppm for methylic protons and four doublets from(CH_3)P=O units in the range 2.1 to 1.6 ppm, which correspond to 24 and 16 protons, respectively. In the DQF-COSY spectrum at the same temperature (Figure S3, Supporting Information) the strongest cross peaks arise from methylene groups. For instance, cross peaks in the aromatic region correspond to protons 3 and 5 (see Scheme 1 for the numbering) for both sets of resonances (δ = 7.52/7.46 ppm and 6.73/6.56 ppm), which points to two different types of phenol rings. The ratio of their integrated intensities (1:1) and the remarkable difference in the chemical shift (Δ = 0.85 ppm) fully back the interpretation that four phosphinoyl arms are coordinated. Moreover, the NOE effect evidenced at 293 K between CH_2P=O (δ =4.58 ppm) and CH_3P=O (δ =1.75 ppm) is consistent with a bent conformation of the phosphinoyl arm at this temperature, at which the unbound octamer is conformationally most labile, again pointing to the coordination of the pendant arms.

The methylene resonances give important information on the conformation of the bound calixarene because the $\Delta\delta$ shifts can be used for differentiating between *sin* or *anti* aromatic protons.[30] Assignment of axial and equatorial protons is dependent on DQF-COSY experiments (Figure 5, Table 2). Three types of resonances from the Ar-CH_2Ar methylene protons (H^a, H^b, H^c) with intensity ratios 6:4:6 are observed at 213 K in the presence of triflate; two of them appear as pairs of doublets (H^a and H^c). The presence of distinct signals for both equatorial and axial protons for every CH_2 group points to a cone-like conformation of the corresponding phenolic units.[32] Comparison of the chemical shift differences ($\Delta\delta$ = ≈ 0.6 for H^a, ≈ 0.1 ppm for H^b and H^c) with those obtained for unbound B_8bL^8 (δ =0.6 ppm) and the anhydrous $[LaB_4bL^4]^{3+}$ complex (δ =0.15 ppm)[17] leads to the assignment of the signals corresponding to the largest $\Delta\delta$ value to the uncoordinated units of the macrocycle. In favour of this assignment is the fact that unusually small $\Delta\delta$ values are observed when a small guest − in our case the lanthanide ion − enters a calixarene cavity.[15] Upon increasing the temperature to 293 K, methylene bridges give rise to four pairs of resonances ($H^{a'}$, $H^{b'}$, $H^{c'}$, $H^{d'}$) in the ratio 4:4:4:4; two of them (H^b, H^c) appear as pairs of doublets whereas the other two (H^a, H^d) feature three components. Finally, two and three signals from CH_2P=O in a ratio 4:4 and 4:2:2 were observed at 213 and

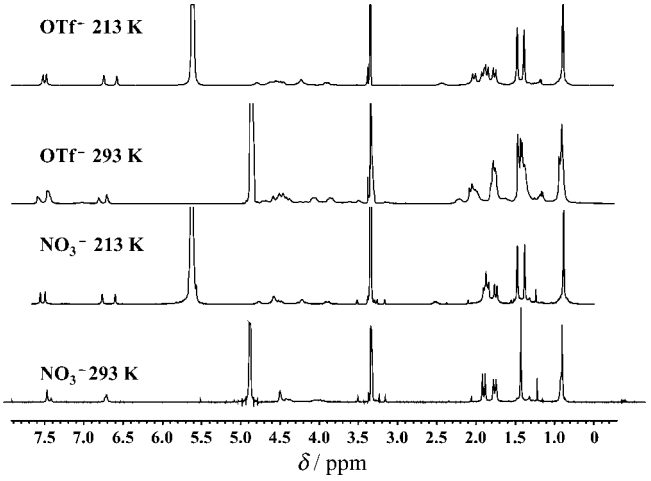

Figure 4. ^1H NMR spectra of a solution of B_8bL^8 (3.3×10^{-3} M) with 1 equiv. of $Lu(OTf)_3{\cdot}9H_2O$ or $Lu(NO_3)_3{\cdot}4H_2O$ in CD_3OD at 213 K and 293 K.

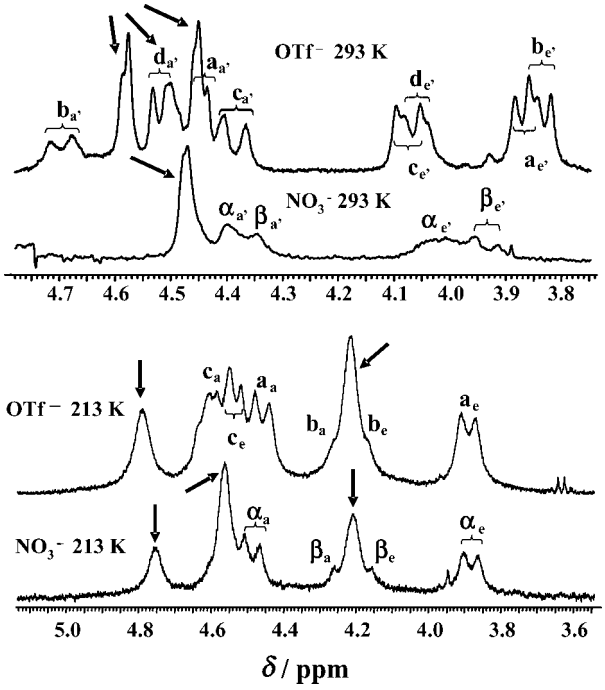

Figure 5. Part of the ^1H NMR spectra of a B_8bL^8 solution (3.3×10^{-3} M) with 1 equiv. of $Lu(OTf)_3{\cdot}9H_2O$ or $Lu(NO_3){\cdot}4H_2O$ in CD_3OD at 213 and 293 K. Arrows point to resonances from the CH_2PO methylene groups.

Table 2. ^{1}H NMR spectroscopic chemical shifts (δ) of the methylene groups of solutions of B_8bL^8 in CD_3OD containing 1 equiv. of $[Lu(Otf)_3]$ or $[Lu(NO_3)_3]$.

T / K	Anion	Proton	δH_{ax} / ppm	*h*e / ppm	$\Delta(H_{ax} - H_{eq})$ / ppm	*I* / a.u.	$\delta CH_2(P{=}O)$ / ppm
213	Otf^-	H^a	4.46	3.88	0.58	6	4.79, 4.22 (4:4)
		H^b	4.26	4.17	0.09	4	
		H^c	4.59	4.53	0.06	6	
293	Otf^-	$H^{a'}$	4.46	3.87	0.59	4	4.58, 4.50, 4.43 (4:2:2)
		$H^{b'}$	4.69	3.83	0.86	4	
		$H^{c'}$	4.38	4.07	0.31	4	
		$H^{d'}$	4.52	4.06	0.46	4	
213	NO_3^-	Hα	4.48	3.89	0.59	5	4.76, 4.57, 4.21 (2:4:2)
		Hβ	4.26	4.16	0.1	3	
293	NO_3^-	Hα′	4.35	3.93	0.42	4	4.47
		Hβ′	4.39	4.02	0.37	4	

293 K, respectively. These data can be interpreted by a proposed structure (Figure 6a) in which coordination occurs through the central four phosphinoyl pendant arms and possibly implies binding by the phenolic units. Interconversion processes through annulus are then more difficult and the NMR spectrum at room temperature features sharper signals. Alternatively, the coordination sphere may be completed by methanol molecules. Because triflate is very weakly coordinating in methanol,[36] it is reasonable to surmise that this counterion only interacts in the second coordination sphere.

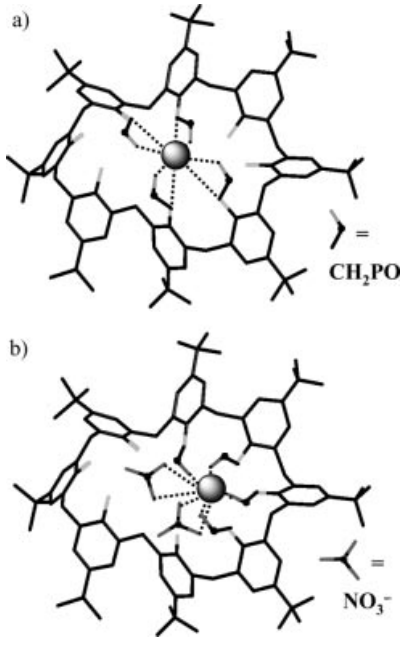

Figure 6. Schematic representation of the possible solution structure of the 1:1 complexes with B_8bL^8 compatible with NMR spectroscopic data: (a) central coordination involving phenolic groups in the case of the triflate, (b) side complexation in the case of the nitrate. Note that phosphinoyl arms are only shown when coordinating, for the sake of clarity.

Next we tested the influence of nitrate, which is more strongly coordinating than triflate,[36] by measuring the spectra of 1:1 solutions of B_8bL^8 and lutetium nitrate at a concentration of 1.9×10^{-3} M. At 213 K, both the 1D (Figure 5) and 2D (Figure S4, Supporting Information) spectra are quite similar to the ones discussed above for lutetium triflate with the exception of the methylene bridge region, which displays only two types of signals instead of three. These signals appear as a pair of doublets (Hα, $\Delta\delta$ = 0.6 ppm) and a singlet (H_β, $\Delta\delta$ = 0.1 ppm) in a ratio 5:3. By comparing the $\Delta\delta$ values with those obtained for lutetium triflate, this ratio may be explained as arising from the presence of three methylene bridges connecting four units of the octamer with coordinated pendant arms (smaller $\Delta\delta$) and five methylene bridges connecting the other four units with uncoordinated arms (larger $\Delta\delta$). In line with this interpretation is the observation of three resonances in a ratio 4:2:2 for the $CH_2(P{=}O)$ methylene groups; in view of the fluxionality of the calix[8]arene, the uncoordinated pendants experience two different chemical environments.

In contrast, the spectrum recorded at 293 K is remarkably different from the one for the triflate complex: much broader and unresolved signals in the methylene region are observed. The two distinguishable pairs of signals from the methylene groups $H^{\alpha'}$ and $H^{\beta'}$ have average $\Delta\delta \approx 0.4$ ppm, which is in line with faster chemical exchanges on the NMR timescale. Only one averaged resonance is seen for the eight $CH_2P{=}O$ units. Interpretation of these data can be made by reference to a complex with the parent *p-tert*-butylcalix[8]arene H_8L^8, $[Eu(H_6L^8)(NO_3)(DMF)_4]$, in which both nitrate and calixarene act as bidentate ligands.[24] In our case, in view of the strong coordinating nature of the pendant arms and of their length and flexibility, one could postulate a "side" coordination as well, but involving one (or two) bidentate nitrate anion(s), as the mono- (85%) and bis(nitrato) (15%) complexes are the predominant species in $Ln(NO_3)_3$ methanol solutions at the concentrations used in this work.[37] Therefore, the above-described data may be interpreted by considering a side coordination of the lutetium ion by four phosphinoyl arms out of the octamer "cavity" (see Figure 6b). The lutetium ion may not be coordinated as deeply in the macrocycle as in the case of the triflate and, as a consequence, methanol molecules may complete the inner coordination sphere or compete with the

phosphoryl and nitrate groups. In such a model, the system is more fluxional relative to the triflate complex, which explains the average $\Delta\delta$ values observed at room temperature. Consequently, the choice of the counterion, triflate or nitrate, allows the final structure of the lanthanide complexes to be tuned: four phosphinoyl arms are bound in each case but the coordination geometry and the cation orientation in the calixarene cavity depend on the counterion used.

Isolation and Characterization of the 1:1 and 2:1 Ln^{III} Complexes

The 1:1 and 2:1 Ln^{III} complexes (Ln = La, Eu, Tb, and Lu) evidenced in solution studies could be isolated from stoichiometric solutions of B_8bL^8 ($\approx 3.4 \times 10^{-3}$ M) and lanthanide triflate or nitrate in methanol. For Eu^{III}, elemental analyses correspond to formulae $Eu(OTf)_3(B_8bL^8)\cdot 13H_2O$ and $Eu_2(B_8bL^8)(NO_3)_6\cdot H_2O$. Unfortunately, no single crystals of X-ray quality could be obtained, despite numerous trials. The ^1H NMR spectra of a methanolic solution of the isolated 1:1 and 2:1 lutetium complexes are similar to the spectra obtained for a solution of B_8bL^8 containing one equivalent of lutetium triflate and nitrate, respectively (Figure S5, Supporting Information). The low solubility of these complexes, particularly the lutetium 2:1 species, required heating the solutions and high dilution; as a consequence, the ^1H NMR spectra contain traces attributed to the free octamer, which reveals partial decomplexation. High resolution MS (FAB) data for 1:1 (Lu) and 2:1 (Tb) complexes in methanol are shown in Table 3 and Figure S6 (Supporting Information). For the bimetallic complex, only peaks corresponding to a 1:1 species are observed, in line with the corresponding NMR spectroscopic data and pointing again to the low stability of the 2:1 species in solution.

Table 3. Molecular peaks and main fragments observed by MS (FAB) analysis of $Lu(B_8bL^8)(OTf)_3\cdot 13H_2O$ and $Tb_2(B_8bL^8)(NO_3)_6\cdot H_2O$.

Ln	Mol.Weight	Species	Obsd. *m/z*	Calcd. *m/z*
Lu	2638.84	$[L + Lu]^{3+}$	730.99	730.66
		$[L + 2H]^{2+}$	1010.03	1009.52
		$[L + H + Na]^{2+}$	1021.02	1020.51
		$[L + H + Na + H_2O]^{2+}$	1029.00	1029.52
		$[L + 2Na + 3H_2O + CH_3OH]^{2+}$	1073.98	1074.53
		$[L + 2Na + 2H_2O + 2CH_3OH]^{2+}$	1080.98	1081.54
		$[L + Lu + OTf]^{2+}$	1170.96	1170.47
		$[2\,L + Lu]^{3+}$	1403.68	1403.00
		$[L + H]^{+}$	2018.06	2018.03
		$[L + Na]^{+}$	2041.04	2040.01
Tb	2520.84	$[L + 6H + 4H_2O + 4CH_3OH]^{6+}$	370.45	370.54
		$[L + 6H + 5H_2O + 4CH_3OH]^{6+}$	373.29	373.54
		$[L + Tb]^{3+}$	725.99	725.31
		$[L + Tb + H_2O]^{3+}$	730.33	731.32
		$[L + Tb + 4H_2O + 2CH_3OH]^{3+}$	770.97	770.68
		$[L + Tb + 6H_2O + CH_3OH]^{3+}$	772.98	772.01
		$[L + 2H + 6H_2O + 3CH_3OH]^{2+}$	1110.98	1111.60
		$[L + Tb + NO_3]^{2+}$	1119.47	1118.97
		$[2\,L + Tb + 7H_2O + 6CH_3OH]^{3+}$	1503.99	1503.74
		$[L + Tb + 2NO_3]^{+}$	2300.00	2299.94

The IR spectra of the 1:1 and 2:1 Eu^{III} complexes (Figure S7, Supporting Information) reveal bathochromic shifts of 25 and 40 cm^{-1}, respectively, relative to that of the free ligand, for the ν(P=O) vibration; these shifts confirm the coordination of the macrocycle by the metal ion. A similar redshift (35 cm^{-1}) was reported for a 1:2 (Ln/L) lanthanide complex with B_4bL^4.[17] Typical vibrations of CH_2 groups are observed in the spectral ranges 750 to 760, 935 to 945 and 1290 to 1295 cm^{-1}, and they are assigned to out-of-plane C–H twisting, rocking and wagging modes, respectively. Anion vibrations were assigned by comparison with $Eu(OTf)_3\cdot 5H_2O$ and $Eu(NO_3)_3\cdot 6H_2O$. The presence of both coordinated and uncoordinated triflate groups is consequently ascertained for the Eu^{III} 1:1 complex. In the 1100 to 1300 cm^{-1} range, higher frequency $\nu(SO_3)$ and $\nu(CF_3)$ modes of this complex overlap to form a broad structured band that remarkably differs from the corresponding bands for the triflate salt. The presence of a coordinated triflate anion is also confirmed by the appearance of $\nu_s(SO_3)$ and $\nu_{as}(SO_3)$ modes at 1028 and 1238 cm^{-1}, respectively.[38] The latter overlaps with the $\nu_s(CF_3)$ mode. Bands at 1280, 1222 and 1164 cm^{-1} are assigned to the $\nu_{as}(SO_3)$, $\nu_s(CF_3)$ and $\nu_{as}(CF_3)$ modes of uncoordinated triflate. In the FIR range, the intense peak at 638 cm^{-1} and the less intense band at 518 cm^{-1} correspond to the $\delta_s(SO_3)$ and $\delta_{as}(SO_3)$ modes. The integral intensity ratio $\delta_s(SO_3)/\delta_{as}(SO_3)$ is 1.6 and 0.9 for the 1:1 complex and triflate salt, respectively. The bands at 570 and 750 cm^{-1} are associated with $\delta_{as}(CF_3)$ and $\delta_s(CF_3)$ but overlap of the latter with δ(CH) vibrations prevents further intensity analysis. The difference in the intensities of the $\delta(SO_3)$ vibrations, as well as the redshift of the $\delta_{as}(SO_3)$ and $\delta_{as}(CF_3)$ bands for the octamer complex in comparison with corresponding bands for europium triflate are compatible with the presence of two uncoordinated triflate anions in the isolated 1:1 complex.

In the IR spectrum of the 2:1 europium nitrato complex, the characteristic nitrate bands appear at 1510 (ν_5), 1280 (ν_1), 1030 (ν_2), 738 and 755 (ν_3) cm^{-1}. The splitting of the two strongest absorptions (ν_5 and ν_1) is ≈ 230 cm^{-1}, which indicates bidentate coordination by the europium ion with a relatively strong metal–nitrate interaction.[39] All the nitrate groups appear to be coordinated by the lanthanide ion as no band from the free NO_3^- was detected.

Raman spectra of the 1:1 and 2:1 complexes are in line with the above analysis. In addition, the lower effective cross-section of the Raman scattering, as measured by the area of the ν(CH) modes, observed for the 2:1 complex, indicates less changes in polarizability relative to the 1:1 complex. Finally, the appearance of the ν(–O–CH_2–) vibration as a doublet with frequencies 1012 and 1028 cm^{-1} in the 1:1 europium complex, relative to a single band at 1012 cm^{-1} for uncoordinated B_8bL^8 may be evidence for coordinated ether O atoms.[17]

Ligand-Centred Photophysical Properties

The absorption spectrum of B_8bL^8 in methanol at 293 K (Figure 7) displays a broad band with a maximum at

43500 cm^{-1} (230 nm, ε = 8995 $M^{-1}cm^{-1}$), assigned to a transition mainly involving orbitals located on the phosphinoyl groups, and a less intense and split band at 37170 and 36230 cm^{-1} (276 and 279 nm, ε = 2910 and 2720 $M^{-1}cm^{-1}$) for transitions mainly located on the phenyl rings. These absorption bands are not affected by the complexation. Finally, a very weak band is observed around 27600 cm^{-1} (360 nm, ε = 110 $M^{-1}cm^{-1}$), which sustains a large bathochromic shift (≈ 3500 cm^{-1}) upon complexation to Ln^{III}. Because the energy of this band is independent of the lanthanide ion, it can be assigned to a transition connected with an intraligand charge transfer (ILCT) state. The latter is seen at 27000 cm^{-1} in the excitation spectrum of a powdered sample of B_8bL^8 at 293 K, in addition to a band centred at 32800 cm^{-1} and attributed to the $^1\pi\pi^*$ level (Figure S8, Supporting Information). The redshift of the ILCT band in the absorption spectra of solutions containing B_8bL^8 and one equivalent of lanthanide salt confirms the complex formation.[40] A similar weak ILCT band was reported at 27030 cm^{-1} in the excitation spectrum of europium benzoate.[41] Moreover, it is known that ILCT energy depends on the position of the carboxylate group in heterocyclic pyridine–carboxylic ligands containing nonbonding electron pairs.[42] According to these data, the large intensity of the ILCT band in complexes with B_8bL^8, as well as its strong redshift upon complexation, are typical of a charge transfer from the phenol ring to the oxygen atom of the phosphinoyl groups. Because the ILCT band of the complexes lies at lower energy and is more intense than the corresponding band for the uncoordinated ligand, the transition dipole moment is larger for the complexes.[43]

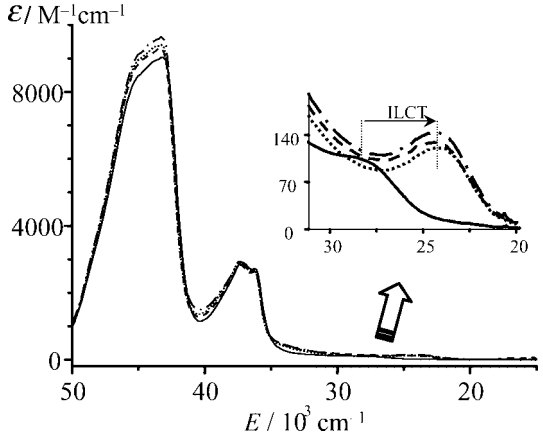

Figure 7. Absorption spectra of B_8bL^8 (1.7 × 10^{-4} M) in MeOH at 293 K (black curves) with 1 equiv. of $Lu(OTf)_3$ (dot), $Eu(OTf)_3$ (dash) and 2 equiv. of $Eu(OTf)_3$ (dash-dot). The inset zooms on the intraligand charge transfer absorption.

According to emission spectra at 77 K, the $^1\pi\pi^*$ state of a powdered sample of the octameric ligand is located at 32800 cm^{-1}. The singlet state energy is not affected by the complexation in the Lu^{III} 1:1 complex but sustains a slight blueshift in the 2:1 complex (+320 cm^{-1}). The triplet state emission occurs at 23600 cm^{-1} for B_8bL^8 and is only seen for the Lu^{III} complexes, for which it is blueshifted by +400 and +130 cm^{-1} for the 1:1 and 2:1 complexes, respectively. It displays a fine structure with vibronic progressions of ≈ 1470 cm^{-1} (1:1) and 1280 cm^{-1} (2:1) which can be attributed to the vibrational mode of the phenol moieties and nitrate groups, respectively (Figure S9, Supporting Information). The luminescence decay associated with the $^3\pi\pi^*$ state of B_8bL^8 is a single exponential function corresponding to a lifetime of 2.61 ms which increases to 3.5–3.6 ms upon complexation. The energy gap $\Delta E(^3\pi\pi^* - {}^1\pi\pi^*)$ amounts to ≈ 8450 and 9150 cm^{-1} (0-phonon transitions) for the investigated 1:1 and 2:1 lutetium complexes, respectively, which is not quite optimum for an efficient ISC.[44] The $^3\pi\pi^*$-to-metal energy transfer efficiency also depends on the energy gap between the feeding triplet state and the accepting Ln^{III} levels. In our case, it appears to be adequate for Tb^{III}, with $\Delta E(^3\pi\pi^* - {}^5D_4)$ ≈ 3600–3800 cm^{-1}, but somewhat less well-suited for Eu^{III}, with $\Delta E(^3\pi\pi^* - {}^5D_0)$ ≈ 6800–7000 cm^{-1}.

The excitation spectra of the luminescent lanthanide complexes contain typical broad bands arising from ligand levels, which confirm the energy transfer from coordinated B_8bL^8 to Ln^{III}, and narrow and characteristic lines from the metal ions. Comparison of the excitation spectra of the 1:1 europium and terbium complexes at 77 K reveals an additional intense broad band centred at 24200 cm^{-1} and expanding to 21400 cm^{-1} in the spectrum of the former, which is assigned to a ligand-to-metal charge transfer (LMCT) band (Figure 8). The strong intensity of this LMCT band is uncommon and could be produced by intensity stealing as the LMCT and ILCT states overlap. A weak band assigned to the LMCT state was also found in the excitation spectrum of the Eu^{III} 2:1 complex with a low-energy edge at 21800 cm^{-1} at 77 K (Figure S10, Supporting Information). The broad band observed in the range 26000 to 28000 cm^{-1} for the 2:1 Tb^{III} complex is assigned to an f–d transition. The optical electronegativity[45] of the ligand in the Eu^{III} 1:1 and 2:1 complexes can be calculated from the energy of the LMCT band and amounts to χ_L = 2.80 and 2.78, respectively. The slightly smaller χ_L value for the 2:1 complex is caused by the presence of coordinated nitrate groups. It has indeed been found for mixed-ligand complexes that ligands with high optical electronegativity

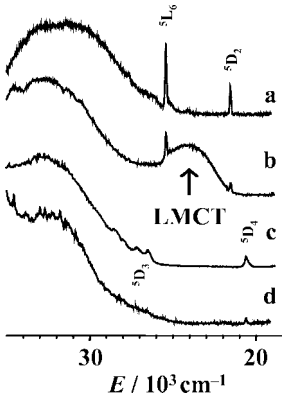

Figure 8. Normalized excitation spectra of the 1:1 powdered complexes with Eu^{III} (a, b) and Tb^{III} (c, d) at 293 K (a, c) and 77 K (b, d). Analysing wavelength set at 612 (Eu^{III}) and 545 (Tb^{III}) nm, respectively.

weaken the metal–ligand interaction of the other ligands with lower χ_L values.[46,47] Therefore, when nitrate, with high optical electronegativity and low polarizability, is coordinated in the 2:1 Eu^{III} complex, the interaction between the metal ion and the calixarene is weakened, henceforth the smaller intensity of the LMCT band. In absence of nitrate, which is the case for the 1:1 complex, the Eu–B_8bL^8 interaction is larger, which leads to a mixing between the ILCT and LMCT states and a concomitant reduction in the efficiency of the excitation of Eu^{III} by the ligand states. Finally, by using the χ_L values found for B_8bL^8, the energy of the LMCT state in the terbium complexes can be estimated to be larger than 51000 cm^{-1}.

Metal-Centred Photophysical Properties in the Solid State

The $^5D_0 \rightarrow {}^7F_J$ transitions of the 1:1 and 2:1 europium complexes recorded at 77 K under broad band excitation display a maximum number of Stark components, which points to low site symmetry (Figure 9; see listing of crystal-field splitting in Table S3, Supporting Information). The integrated intensities of the $^5D_0 \rightarrow {}^7F_J$ transitions relative to $^5D_0 \rightarrow {}^7F_1$, 0.06, 2.28, 0.14 (1:1 complex) and 0.09, 2.55, 0.34 (2:1 complex) for J = 0, 2, 4, respectively, are similar for the two types of complexes.

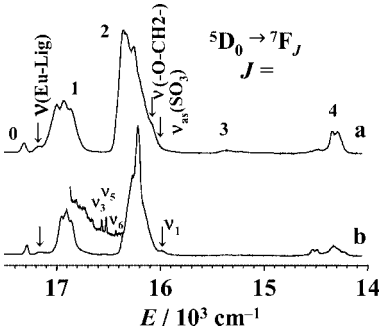

Figure 9. Luminescence spectra of 1:1 (a) and 2:1 (b) europium complexes at 77 K.

Data relevant to the 2:1 complex will first be discussed. The excitation profile of the $^5D_0 \leftarrow {}^7F_0$ transition obtained upon monitoring the $^5D_0 \rightarrow {}^7F_2$ transition (Figure S11, Supporting Information) is symmetric, narrow (full width at half height, fwhh = 7.6 cm^{-1}), and occurs at 17254 cm^{-1} at room temperature and at 17242 cm^{-1} at 10 K. This points to a very similar chemical environment for the two Eu^{III} ions, a fact which is further ascertained by the identical emission spectra obtained upon selective laser excitation through the 0–0 band profile (Figure S12, Supporting Information). Moreover, emission from the Eu($^5D_1$) level could also be obtained at 10 K, which is typical of nitrato complexes (Figure S13, Supporting Information). A number of vibronic satellites related to ligand vibrations and associated with the $^5D_0 \rightarrow {}^7F_J$ (J = 0, 1, and 2) transitions are observed in both excitation and emission spectra. At 10 K, we denote the following satellites (see Figure 9): (1) ν(Eu–Lig) with frequencies 195 and 405 cm^{-1} in the range 17400 to 16850 cm^{-1}, (2) $\nu_5(NO_3^-)$, $\nu_3(NO_3^-)$ and $\nu_6(NO_3^-)$ around ca. 705, 740 and 820 cm^{-1}, respectively, in the range 16420 to 16530 cm^{-1}, (3) vibronic repetition of the $^5D_0 \rightarrow {}^7F_1$ transition with frequency 195 cm^{-1} in the range 16800 to 16450 cm^{-1}, (4) two stretching vibrations $\nu_1(NO_3^-)$ with frequencies 1280 and 1315 cm^{-1} attributed to nonequivalent nitrates, in the range 15960 to 15930 cm^{-1}. In the excitation spectrum, vibronic sidebands appear on the $^5D_2 \leftarrow {}^7F_0$ transition with frequencies 200 (Ln–Lig), 670 (δ_{ring}), 940 (out-of-plane C–H rocking mode), 1020 [ν(–O–CH_2–)], 1120 [ν(P=O)] and 1480 cm^{-1} (ν_{ring}). These data confirm the coordination of the P=O groups, which is in line with ES-MS, NMR, and IR data; they also indicate the presence of different types of coordinated nitrate groups. Furthermore, the luminescence decays of the Eu($^5D_0$) and Tb($^5D_4$) levels are single exponential functions (Table 4). They are long enough to ascertain the absence of water molecules in the inner coordination sphere of the lanthanide ion, the latter is protected from such an interaction by the coordination of nitrate ions. The lifetimes vary only slightly with temperature, which points to a small influence of temperature-dependent nonradiative deactivation processes.

Table 4. Lifetimes (ms) of the metal-centred luminescence upon ligand excitation of powdered samples of Eu^{III} and Tb^{III} 1:1 and 2:1 complexes with B_8bL^8 in the solid state (ss) and of a 2×10^{-3} M solutions (sol) in methanol (ν_{exc} = 37040 cm^{-1}). Standard deviations are given in parentheses.

T/K	Sample	Eu 1:1 (OTf)	Eu 1:1 (NO_3)	Eu 2:1 (NO_3)	Tb 1:1 (OTf)	Tb 1:1 (NO_3)	Tb 2:1 (NO_3)
10	ss	1.27(1), 72% 0.39(1), 38%		1.62(3)	–		–
77	ss	1.18(4)		1.38(2)	1.35(2)		1.93(4)
	sol	1.11(1), 62% 0.5(3), 38%	1.28(4)		1.72(2)	1.72(2)	
295	ss	1.09(2) 53% 0.22(3), 47%		1.29(1)	1.59(1)		1.66(3)
	sol	0.93(2), 58% 0.30(2), 42%	1.10(2)		1.52(3)	1.66(3)	

Relative to the 2:1 complex, the $^5D_0 \leftarrow {}^7F_0$ transition of the 1:1 species is broader (fwhh ≈ 38 cm^{-1}) and weaker. It has a maximum around 17280 cm^{-1} at 293 K and features at least three distinct components separated by about 20 cm^{-1}. Such large energy differences point to the presence of differently coordinated europium ions. The analysis could not, however, be pursued further; the very small intensity of the 0–0 transition prevented the selective laser excitation of the various components. Luminescence lifetime data (Table 4) shed more light on the potential Eu^{III} species present in the complex. While data recorded under low resolution reflect one averaged lifetime for both Eu^{III} and Tb^{III}, high-resolution conditions used for Eu^{III} led to double exponential functions. The longer lifetime, which contributes 60–70% to the decay, corresponds to an Eu^{III} environment devoid of O–H vibrations, whereas the shorter lifetime corresponds to a metal ion bound to water molecules. Assuming that the extra quenching corresponding to the shorter lifetime

only arises from coordinated water molecules, which is reasonable in view of the elemental analysis, an average hydration number $q \approx 2$ can be estimated. As a result, interpretation of both the $^5D_0 \leftarrow ^7F_0$ excitation profile and the lifetime data leads to postulate that two of the three coordination environments have the same hydration number $q \approx 2$, whereas the third environment has $q \approx 0$. This model is feasible in view of the large conformational mobility of the macrocycle and interaction with triflate anions, as shown below. Vibration satellites are also found in the luminescence spectrum of the Eu^{III} 1:1 complex at 10 K: (1) ν(Eu–Lig) with frequencies 107 and 195 cm^{-1} in the range 17160 to 17070 cm^{-1}, (2) $\nu_{as}(SO_3)$ and $\nu_s(CF_3)$ vibrations with frequencies 1260 and 1180 cm^{-1}, respectively (16000–16090 cm^{-1}), (3) a line with frequency 1025 cm^{-1} (16240–16040 cm^{-1}) which is a superposition of $\nu_{as}(SO_3)$ and ν(C–O–CH_2–) vibrational modes. The appearance of vibronic satellites corresponding to triflate vibrations ascertains coordination to the europium ion. The presence of two lower frequency ν(Eu–Lig) satellites is in line with the biexponential lifetime obtained and confirms the presence of at least two different chemical environments for Eu^{III}. Moreover, lines with frequencies 200 (Eu–Lig), 638 (OTf^-), 765 (out-of-plane C–H twist) and 1140 cm^{-1} [ν(P=O)] appear in the excitation spectrum at 77 K as vibronic sidebands of the $^5D_2 \leftarrow ^7F_0$ transition. The presence of the second and fourth lines points to the simultaneous coordination of triflate and phosphinoyl arms of the calixarene. The comparatively large intensity of the vibronic sidebands of the $^5D_0 \rightarrow ^7F_2$ electronic transition in both 1:1 and 2:1 complexes is caused by a resonant vibronic effect in which intensity is borrowed from neighbouring electronic transitions.[48] The intensity of the vibronic interaction is slightly higher in the 1:1 complex, which is judged from the integral intensity of the $^5D_0 \rightarrow ^7F_2$ vibronic sidebands normalized to the intensity of the Stark components of this transition. This observation is in agreement with the presence of a LMCT state in the latter complex and with all the previously discussed data regarding the coordination mode of B_8bL^8 in 1:1 complexes.

Metal-Centred Photophysical Properties in Solution

The luminescence decay of an equimolar solution of europium triflate and B_8bL^8 in methanol is biexponential with lifetimes similar to those determined for the powdered 1:1 sample (Table 4). In addition, the emission spectra of these two samples are very alike (Figure S14, Supporting Information). This is in line with NMR and MS data and points to a solution structure of the complex similar to the solid state one. In contrast, a single exponential decay with a lifetime slightly shorter than the one for the powdered 2:1 sample is observed for the equimolar solution of europium nitrate and B_8bL^8. The emission spectra of this solution and of a powdered 2:1 sample are quite different: (1) the frequency of the ν(Eu–Lig) vibronic satellite is ≈ 10 cm^{-1} larger in solution, (2) the Stark components of the hypersensitive $^5D_0 \rightarrow ^7F_2$ transition are very different and (3) the relative intensity of the $^5D_0 \rightarrow ^7F_0$ transition is larger in solution. These data could be explained by a transformation of the 1:1 complex into a 2:1 species upon crystallization, as observed with other calix[8]arenes,[22] whereas an inverse 2:1→1:1 transformation occurs upon dissolution.

The absolute quantum yield of the metal-centred luminescence upon ligand excitation for B_8L^8 solutions containing one equivalent of $Eu(OTf)_3$ or $Tb(OTf)_3$ in methanol at 293 K is equal to 0.23 and 0.70%, respectively. These low values could be caused by high-energy vibration quenching in addition to a relatively inefficient intersystem crossing process. The quantum yields are somewhat smaller for the solutions containing nitrate, 0.18% (Eu) and 0.53% (Tb). It is worth noting that the powdered 2:1 europium complex has a much higher luminescence intensity than the 1:1 complex.

Conclusions

The results reported here allow us to discuss the influence of the calixarene size on the complexation properties toward lanthanide ions. The smallest calix[4]arene analogue, B_4bL^4, exists in the cone conformation in organic solution and forms stable 1:1 and 1:2 complexes with Ln^{III} ions ($\log\beta_1 \approx 11$ and $\log\beta_2 \approx 20$ in acetonitrile).[17] When the size is increased to yield B_6bL^6, the larger flexibility of the macrocyclic host is reflected in an alternate *in–out* conformation, but complexes with the same stoichiometry form, with similar stability ($\log\beta_1 \approx 10$ and $\log\beta_2 \approx 20$ in acetonitrile).[19] With the larger octamer B_8bL^8, the major species that forms in methanol (solubility problems prevented the study in acetonitrile) has a 1:1 stoichiometry, whereas the 1:2 species is hardly detected; a minor 2:1 species also forms and can be isolated in the solid state. Observation of the latter species is consistent with the bimetallic complexes usually isolated with calix[8]arenes but only in the presence of a nitrate counterion because of its bidentate chelating mode. However, the strong coordination ability of the phosphinoyl groups toward lanthanide ions tends to equalize the ligand–Ln^{III} interaction in the 1:1 species with the three receptors ($\log K_{11} \approx 7$ in methanol for B_8bL^8 compares favourably with $\log\beta_1 \approx 10$ in acetonitrile for the other macrocycles). With respect to the complexes with B_6bL^6, the photophysical properties appear to be less interesting, but they were recorded in a more polar solvent, methanol versus acetonitrile, which prevents strict comparison. However, they are better than with the smallest macrocyclic host, B_4bL^4, at least as far as Eu^{III} is concerned. In addition, a correlation was observed between the optical electronegativities of the ligands and the luminescence efficiency, in relationship with the energy of the LMCT states in lanthanide complexes with the investigated calix[8]arene. The coordination ability and optical electronegativity of the counterion used can be considered as an instrument for assembling lanthanide complexes with a predetermined structure. This opens perspectives for the molecular design of new luminescent lanthanide systems with inequivalent ligands. With these

data at hand, we are now testing the extraction and separation capabilities of the three calixarene receptors towards both lanthanide and actinide cations.[20]

Experimental Section

Starting Materials and General Procedures: All reagents and solvents were of analytical grade and were used without further purification. Chloro(dimethylphosphinoyl)methane was purchased from Hoechst AG (Germany). Stock solutions of lanthanides were made in freshly boiled, doubly distilled water from the corresponding nitrates and triflates, $Ln(NO_3)_3{\cdot}xH_2O$ (x = 3, 4) and $Ln(OTf)_3{\cdot}xH_2O$ (Ln = La, Eu, Tb, Lu; x = 6–10), prepared from their oxides (Rhône–Poulenc, 99.99%) in the usual way.[49] Concentrations of the solutions were determined by complexometric titrations using a standardized Na_2H_2EDTA solution in urotropine buffered medium and with xylenol orange as indicator.[50] Elemental analyses were performed by the Ilse Beetz Laboratory (96301 Kronach, Germany). ESMS spectra were measured with a Finnigan SSQ 710C spectrometer by using a capillary temperature of 200 °C and acceleration potential of 4.5 kV; 10^{-5}–10^{-4} M solutions of the free ligand or its complexes dissolved in methanol were infused in a mixture of $CH_3CN/H_2O/HCOOH$ (50:50:1) for the ligand, or pure CH_3OH for the complexes. High resolution MS (FAB) spectra were recorded with an FTMS 4.7T BioApex II spectrometer from Bruker by the MS-Service unit of the University of Fribourg (Switzerland).

5,11,16,23,29,35,41,47-Octa-*tert*-butyl-49,50,51,52,53,54,55,56-octakis(dimethylphosphinoylmethyleneoxy)calix[8]arene (B_8bL^8): A warm solution of chloro(dimethylphosphinoyl)methane (9.24 g, 73.05 mmol) in xylene (20 mL) was added to fine suspension of octasodium derivative of *p*-*tert*-butylcalix[8]arene in refluxing xylene. The latter was prepared by the addition of Na (0.64 g, 27.89 mmol) to a mixture of *p*-*tert*-butylcalix[8]arene (2.26 g, 1.74 mmol), MeOH (70 mL) and xylene (200 mL), followed by distillation of MeOH and part of the xylene. The resulting mixture was heated at reflux and stirred under an atmosphere of nitrogen for 97 h. After cooling to 50–60 °C, the mother liquor was separated by centrifugation, and the precipitate was washed with warm (40–50 °C) xylene (5 × 25 mL) and dichloromethane (150 mL, stirring at room temp. for 2 h). After filtration, the white solid residue (3.73 g) was washed with distilled water (8 × 60 mL), separated by centrifugation and redissolved in MeOH (200 mL). Concentrated HCl (2 mL) was added, the transparent colourless methanol solution was filtered and methanol was evaporated. The residue was washed with water (7 × 80 mL), dried and recrystallised from DMF to give a white solid (1.74 g, 49.5%). B_8bL^8 does not melt until 300 °C and is soluble at room temp. in MeOH, EtOH, 2-propanol and chloroform and sparingly soluble at elevated temperatures in DMSO, DMF and acetonitrile; B_8bL^8 is insoluble in water, aromatic and aliphatic hydrocarbons (heptane, toluene, xylene), acetone, diethyl ether, THF, acetic acid and diisopropyl ether. It can be recrystallised from DMF, DMSO, and acetonitrile. ^{1}H NMR (400 MHz, [D$_6$]DMSO): δ = 6.98 (s, 16 H, Ar-H), 4.04 (s, 16 H, Ar-CH_2-Ar), 3.97 (s, 16 H, CH_2P=O), 1.36 [d, $^2J_{HP}$ = 9.2 Hz, 48 H, $(CH_3)_2$PO], 1.04 (s, 72 H, C$(CH_3)_3$]) ppm. ^{1}H NMR (400 MHz, CD_3OD, 293 K): δ = 7.07 (s, 16 H, Ar-H), 4.16 (s, 16 H, Ar-CH_2-Ar), 4.15 (d, $^2J_{HH}$ = 5.64 Hz, 16 H, CH_2P=O), 1.59 [d, $^2J_{HP}$ = 13.32 Hz, 48 H, $(CH_3)_2$P=O], 1.13 (s, 72 H, C$(CH_3)_3$]) ppm. ^{31}P{^{1}H} NMR (161.9 MHz, [D$_6$]DMSO): δ = 39.8 ppm. ^{13}C NMR (100.6 MHz, $CDCl_3$): δ = 153.2 (d, $^3J_{CP}$ = 11.3 Hz, Ar-*i*), 147.6(s, Ar-*o*), 132.0 (s, Ar-*m*), 126.7 (s, Ar-*p*), 71.5 (d, J_{CP} = 80 Hz, CH_2P=O), 34.7(s, tert. C), 31.8 (CH_3-*tert*), 29.9 (s, Ar-CH_2-Ar), 14.9 (d, J_{CP} = 68.3 Hz, CH_3P=O) ppm. IR (KBr disk): $\tilde{\nu}$ = 1171 (P=O) cm^{-1}. ESMS: m/z = 1009.98 [B_8bL^8 + 2H]$^{2+}$, 2018.35 [B_8bL^8 + H]$^{1+}$, 2040.95 [B_8bL^8 + Na]$^{1+}$. IR: $\tilde{\nu}$ = 1160 and 1173 (P=O) cm^{-1} (before and after heating for 20 h at 413 K). Raman: ν_{ring} 1592, 1112 cm^{-1}; breathing mode of phenol ring 1008 cm^{-1} for $B_8bL^8{\cdot}5H_2O$. $C_{112}H_{184}O_{24}P_8$ (= $B_8bL^8{\cdot}8H_2O$) (2162.44): calcd. C 62.21, H 8.58, P 11.46; found C 62.34, H 8.99, P 11.42.

1:1 Complexes: A methanolic solution (3 mL) of B_8bL^8 (0.0215 g, 0.0102 mmol) was heated at 60 °C and a solution of $Ln(OTf)_3{\cdot}xH_2O$ (Ln = La, x = 10; Eu, x = 7; Tb, x = 6; Lu, x = 9; 0.0106 g, 0.0142 mmol for Eu) in MeOH (1.75 mL) was slowly added. A precipitate appeared, and the mixture was stirred for 2 h under an atmosphere of nitrogen at 60 °C. The precipitate was centrifuged, washed repeatedly with MeOH and dried for 48 h at 60 °C and 10^{-2} Torr. All compounds are extremely hygroscopic yellow powders. Yields: 62 (La), 58 (Eu), 44 (Tb) and 72% (Lu). $Eu(B_8bL^8)(OTf)_3{\cdot}13H_2O$ (2851.72): calcd. C 48.44, H 6.86, O 21.32, P 8.69, S 3.37; found C 47.43, H 6.26, O 26.15, P 9.02, S 3.51. Formulae of the other complexes were established by ^{1}H and ^{31}P{^{1}H} NMR spectroscopy. HRMS (FAB): m/z = 723.20 [$Eu(B_8bL^8)$]$^{3+}$, 730.99 [$Lu(B_8bL^8)$]$^{3+}$, experimental isotopic distribution patterns matched the calculated ones (Figure S5, Supporting Information). IR: $\tilde{\nu}$ = 1130 (P=O), shift 7, 2, 3 and 9 cm^{-1} for La, Eu, Tb, and Lu, respectively; 635 cm^{-1} (OTf^-), shift 1, 2, 1 and 2 for La, Eu, Tb, and Lu, respectively. Raman: ν_{ring} 1592, 1112 cm^{-1}; breathing mode of phenol ring 1012, 1028 cm^{-1} for $Tb(B_8bL^8)$ $(OTf)_3{\cdot}13H_2O$.

2:1 Complexes: A MeOH solution (4 mL) of B_8bL^8 (0.0226 g; 0.0107 mmol) was heated at 60 °C, and a solution of $Ln(NO_3)_3{\cdot}xH_2O$ (0.0912 g; 0.0222 mmol for Eu; Ln = La, x = 4; Eu, x = 4; Tb, Lu, x = 3) in MeOH (1.4 mL) was added dropwise. A precipitate appeared, and the mixture was stirred for 4 h under an atmosphere of nitrogen at 60 °C. The precipitate was centrifuged, washed with MeOH (2×6 mL) and dried for 48 h at 60 °C and 10^{-2} Torr. All the compounds appeared as white hygroscopic powders. Yields: 58 (La), 52 (Eu), 48 (Tb) and 64% (Lu). $Eu_2(B_8bL^8)(NO_3)_6{\cdot}H_2O$ (2712.32): calcd. C 49.60, H 6.32, O 20.62, P 9.13, N 3.10; found C 51.52, H 6.35, O 15.30, P 9.38, N 2.18. Formulae of the other complexes were established by ^{1}H and ^{31}P{^{1}H} NMR experiments. HRMS (FAB): m/z = 723.28 [$Eu(B_8bL^8)$]$^{3+}$, 725.99 [$Tb(B_8bL^8)$]$^{3+}$, experimental isotopic distribution patterns matched the calculated ones. IR: $\tilde{\nu}$ = 1115 (P=O), shift 3, 5 and 10 cm^{-1} for Eu, Tb and Lu, respectively; 735 (NO_3^-), shift 3, 5 and 8 cm^{-1} for Eu, Tb and Lu. Raman: ν_{ring} 1592, 1112 cm^{-1}; breathing mode of phenol ring 1036 cm^{-1} for $Lu_2(B_8bL^8)$ $(NO_3)_6{\cdot}H_2O$.

Analytical and Physicochemical Measurements: UV/Vis absorption spectra were measured with a Perkin–Elmer Lambda 900 spectrometer with the use of quartz Suprasil® cells of 0.2- and 1-cm path length. Reflectance IR spectra were obtained from powdered samples with a Perkin–Elmer Spectrum One FTIR spectrometer. FIR spectra were recorded with an IFS 13v FTIR spectrometer from Bruker equipped with a pyroelectric DTGS detector. Raman spectra were obtained by means of a Spex 1403 spectrometer with RCA photomultiplier and an argon laser Stabilite 2017 from Spectra-Physics. 1D ^{1}H and ^{31}P{^{1}H} NMR experiments as well as 2D DQF-COSY and ROESY experiments were performed with a Bruker Avance DRX 400 spectrometer. Chemical shifts are given in ppm relative to TMS. All spectra were recorded in CD_3OD (99.9%, Aldrich). Spectrophotometric titrations were performed on a J&M diode-array spectrometer (Tidas series) connected to an external computer in a thermostatted (25.0 ± 0.1 °C) glass-jacketed vessel

with quartz cells of 0.100 cm path length. In a typical experiment, B_8bL^8 (10^{-4} M; 12 mL) was titrated with solutions of the Ln^{III} salt (10^{-3} M); the titrant (0.1 mL) was added by means of a Socorex® micropipette, and spectra were measured after 5 min to equilibrate the solution. The solvent used (MeOH) was of spectroscopic grade (Fluka AG, Buchs, Switzerland). Factor analysis[51] and mathematical treatment of the spectrophotometric data were performed with the SPECFIT[52,53] program.

Low-resolution luminescence measurements (spectra and lifetimes) were recorded with a Fluorolog FL 3–22 spectrometer from Spex-Jobin–Yvon-Horiba at 293 and 77 K and corrected for the instrumental function. Emission and excitation spectra of solutions were measured in 1-cm path length quartz Suprasil cell. The temperature was kept constant by using a FL-1027 thermostatted cell holder connected to a water bath. Phosphorescence lifetimes (τ, averages of at least three measurements) were measured by using a quartz capillary, monitoring the maxima of the emission spectra, and enforcing a 0.05 ms delay. The decays were analysed with Origin 7.0. Quantum yields of Eu^{III}- and Tb^{III}-centred luminescence were determined relative to those of the corresponding tris(dipicolinates) in 0.2-cm Quartz Suprasil cells.[54] The refractive indices were 1.333 for solutions in water and 1.3288 for solutions in MeOH, λ_{exc} = 279 (ref. A = 0.1938) and 276 (sample, A = 0.1911) nm; a filter (320 nm) was inserted to eliminate Raleigh diffusion and second order spectra. High resolution laser-excited luminescence spectra and lifetimes were measured by using published procedures.[55]

Supporting Information (see footnote on the first page of this article): Additional tables of the MS spectrum analysis of B_8bL^8 containing different equivalents of $Eu(OTf)_3{\cdot}7H_2O$ or $Eu(NO_3)_3{\cdot}4H_2O$, ^1H, DQF-COSY and ROESY NMR spectroscopic data of the Lu complexes and their HRMS (FAB) spectra. IR and luminescence data of the europium complexes.

Acknowledgments

This work is supported by the Swiss Federal Office for Research (COST Action D18, contract C00.0030/506 250). We thank Daniel Baumann for the FIR and Raman spectra and Frédéric Gumy for his help in acquiring the photophysical data.

[1] Z. Asfari, V. Böhmer, J. M. Harrowfield, J. Vicens, *Calixarenes* (Eds.: Z.Asfari, V.Böhmer, J. M.Harrowfield, J.Vicens), Kluwer Academic Publishers, Dordrecht, **2001**.
[2] G. J. Lumetta, R. D. Rogers, A. Gopalan (Eds.) *Calixarenes for Separations*, ACS Symposium Series, American Chemical Society, Washington D. C., **2000**, vol. 757.
[3] F. Sansone, M. Fontanella, A. Casnati, R. Ungaro, V. Böhmer, M. Saadioui, K. Liger, J. F. Dozol, *Tetrahedron* **2006**, *62*, 6749–6753.
[4] F. Arnaud-Neu, J. K. Browne, D. Byrne, D. J. Marrs, M. A. McKervey, P. O'Hagan, M.-J. Schwing-Weill, A. Walker, *Chem. Eur. J.* **1999**, *5*, 175–186.
[5] C. D. Gutsche, *Calixarenes Revisited: Monographs in Supramolecular Chemistry*, (Ed.: J. F.Stoddart), The Royal Society of Chemistry, Cambridge, **1998**.
[6] P. D. Beer, J. Cadman, *Coord. Chem. Rev.* **2000**, *205*, 131–155.
[7] J. L. Atwood, L. J. Barbour, M. J. Hardie, C. L. Raston, *Coord. Chem. Rev.* **2001**, *222*, 3–32.
[8] C. B. Smith, L. J. Barbour, M. Makha, C. L. Raston, A. N. Sobolev, *Chem. Commun.* **2006**, 950–952.
[9] S. E. Matthews, P. Schmitt, V. Felix, M. G. B. Drew, P. D. Beer, *J. Am. Chem. Soc.* **2002**, *124*, 1341–1353.
[10] D. R. Stewart, C. D. Gutsche, *J. Am. Chem. Soc.* **1999**, *121*, 4136–4146.
[11] F. Cunsolo, G. M. L. Consoli, M. Piattelli, P. Neri, *Tetrahedron Lett.* **1996**, *37*, 715–718.
[12] T. Kajiwara, K. Katagiri, M. Hasegawa, A. Ishii, M. Ferbinteanu, S. Takaishi, T. Ito, M. Yamashita, N. Iki, *Inorg. Chem.* **2006**, *45*, 4880–4882.
[13] J.-C. G. Bünzli, F. Besançon, F. Ihringer in *Calixarenes for Separations* (Eds.: G. J. Lumetta, R. D. Rogers, A. Gopalan), American Chemical Society, Washington D. C., **2000**, vol. 757, ch. 14, pp. 179–194, and references therein.
[14] C. B. Dieleman, C. Loeber, D. Matt, A. De Cian, J. Fischer, *J. Chem. Soc., Dalton Trans.* **1995**, 3097–3100.
[15] C. B. Dieleman, D. Matt, P. G. Jones, *J. Organomet. Chem.* **1997**, *546*, 461–473.
[16] M. R. Yaftian, M. Burgard, D. Matt, C. Wieser-Jeunesse, C. B. Dieleman, *J. Incl. Phenom. Mol. Recognit. Chem.* **1997**, *27*, 127–140.
[17] L. Le Saulnier, S. Varbanov, R. Scopelliti, M. Elhabiri, J.-C. G. Bünzli, *J. Chem. Soc., Dalton Trans.* **1999**, 3919–3925.
[18] V. Videva, A.-S. Chauvin, S. Varbanov, C. Baux, R. Scopelliti, M. Mitewa, J.-C. G. Bünzli, *Eur. J. Inorg. Chem.* **2004**, 2173–2179.
[19] F. d. M. Ramirez, S. Varbanov, C. Cécile, G. Muller, N. Fatin-Rouge, R. Scopelliti, J.-C. G. Bünzli, *J. Chem. Soc., Dalton Trans.* **2002**, 4505–4513.
[20] F. d. M.Ramirez, S.Varbanov, J. P.Padilla, J.-C. G.Bünzli, unpublished work, **2006**.
[21] P. Neri, G. M. L. Consoli, F. Cunsolo, C. Geraci, M. Piattelli, *New J. Chem.* **1996**, *20*, 433–446.
[22] J.-C. G. Bünzli, F. Besançon, *Phys. Chem. Chem. Phys.* **2005**, *7*, 2191–2198, and references therein.
[23] J. M. Harrowfield, M. I. Ogden, A. H. White, *Aust. J. Chem.* **1991**, *44*, 1249–1262.
[24] J. M. Harrowfield, M. I. Ogden, W. R. Richmond, A. H. White, *J. Chem. Soc., Dalton Trans.* **1991**, 2153–2160.
[25] J.-C. G. Bünzli, F. Ihringer, *Inorg. Chim. Acta* **1996**, *246*, 195–205.
[26] J.-C. G. Bünzli, F. Ihringer, P. Dumy, C. Sager, R. D. Rogers, *J. Chem. Soc., Dalton Trans.* **1998**, 497–504.
[27] A. Casnati, S. Barboso, H. Rouquette, M. J. Schwing-Weill, F. Arnaud-Neu, J. F. Dozol, R. Ungaro, *J. Am. Chem. Soc.* **2001**, *123*, 12182–12190.
[28] M. M. Mark, C. H. Dungan, M. M. Grutchfield, J. R. van Wazer in *Topics in Phosphorous Chemistry, Compilation of ^{31}P NMR Data* (Eds.: M. Grayson, E. J. Griffith), John Wiley & Sons, New York, **1967**, vol. 5, pp. 227–475.
[29] C. Wieser-Jeunesse, D. Matt, M. R. Yaftian, M. Burgard, J. M. Harrowfield, *C. R. Acad. Sci. Paris, Ser. IIc* **1998**, *1*, 479–502.
[30] S. Kanamathareddy, C. D. Gutsche, *J. Org. Chem.* **1994**, *59*, 3871–3879.
[31] C. Jaime, J. de Mendoza, P. Prados, P. M. Nieto, C. Sanchez, *J. Org. Chem.* **1991**, *56*, 3372–3376.
[32] C. D. Gutsche, B. Dhawan, J. A. Levine, K. Hyun No, L. J. Bauer, *Tetrahedron* **1983**, *39*, 409–426.
[33] R. G. Janssen, J. P. M. Vanduynhoven, W. Verboom, G. J. vanhummel, S. Harkema, D. N. Reinhoudt, *J. Am. Chem. Soc.* **1996**, *118*, 3666–3675.
[34] H. Otsuka, K. Araki, T. Sakaki, K. Nakashima, S. Shinkai, *Tetrahedron Lett.* **1993**, *34*, 7275–7278.
[35] J. P. M. van Duynhoven, R. G. Janssen, W. Verboom, S. M. Franken, A. Casnati, A. Pochini, R. Ungaro, J. de Mendoza, P. M. Nieto, P. Prados, D. N. Reinhoudt, *J. Am. Chem. Soc.* **1994**, *116*, 5814–5822.
[36] J.-C. G. Bünzli, A. E. Merbach, R. M. Nielson, *Inorg. Chim. Acta* **1987**, *139*, 151–152.
[37] J.-C. G. Bünzli, A. Milicic-Tang "Solvation and Anion Interaction in Organic Solvents" in *Handbook on the Physics and Chemistry of Rare Earths*, Elsevier, Amsterdam, **1995**, vol. 21. ch.145.

[38] P. Di Bernardo, G. R. Choppin, R. Portanova, P. L. Zanonato, *Inorg. Chim. Acta* **1993**, *207*, 85–91.
[39] K. Nakamoto, *Infrared and Raman Spectra of Inorganic and Coordination Compounds Part A: Theory and Applications in Inorganic Chemistry*, Wiley, New York, **1997**.
[40] J.-M. Lehn in *Frontier in Supramolecular Organic Chemistry and Photochemistry* (Eds.: H.-J. Schneider, H. Dürr), VCH, Weinheim, **1991**, pp. 1–28.
[41] V. Tsaryuk, V. Zolin, J. Legendziewicz, *J. Lumin.* **2003**, *102*, 744–750.
[42] V. F. Zolin, L. N. Puntus, V. I. Tsaryuk, V. A. Kudryashova, J. Legendziewicz, P. Gawryszewska, R. Szostak, *J. Alloys Compd.* **2004**, *380*, 279–284.
[43] J. D. Lewis, J. N. Moore, *Dalton Trans.* **2004**, 1376–1385.
[44] F. J. Steemers, W. Verboom, D. N. Reinhoudt, E. B. Vandertol, J. W. Verhoeven, *J. Am. Chem. Soc.* **1995**, *117*, 9408–9414.
[45] C. K. Jorgensen, *Mol. Phys.* **1962**, *5*, 271–277.
[46] V. Tsaryuk, I. Turowska-Tyrk, J. Legendziewicz, V. Zolin, R. Szostak, L. N. Puntus, *J. Alloys Compd.* **2002**, *341*, 323–332.
[47] V. Tsaryuk, J. Legendziewicz, L. N. Puntus, V. Zolin, J. Sokolnicki, *J. Alloys Compd.* **2000**, *300*, 464–470.
[48] V. D. Savchenko, V. I. Tsaryuk, V. F. Zolin, Yu. K. Gusev, *Proc. SPIE-Int. Soc. Opt. Eng.* **1996**, *2706*, 134–141.
[49] J. F. Desreux in *Lanthanide Probes in Life, Chemical and Earth Sciences – Theory and Practice* (Eds.: J.-C. G. Bünzli, G. R. Choppin), Elsevier, Amsterdam, **1989**, ch. 2, pp. 43–64.
[50] G. Schwarzenbach, *Complexometric Titrations*, Chapman & Hall, London, **1957**.
[51] E. R. Malinowski, D. G. Howery, *Factor Analysis in Chemistry*, John Wiley, New York, **1991**.
[52] H. Gampp, M. Maeder, C. J. Meyer, A. D. Zuberbühler, *Talanta* **1985**, *32*, 257–264.
[53] H. Gampp, M. Maeder, C. J. Meyer, A. D. Zuberbühler, *Talanta* **1986**, *33*, 943–951.
[54] A.-S. Chauvin, F. Gumy, D. Imbert, J.-C. G. Bünzli, *Spectrosc. Lett.* **2004**, *37*, 517–532; Erratum: A.-S. Chauvin, F. Gumy, D. Imbert, J.-C. G. Bünzli, *Spectrosc. Lett.* **2007**, *40*, 193.
[55] R. Rodriguez-Cortinas, F. Avecilla, C. Platas-Iglesias, D. Imbert, J.-C. G. Bünzli, A. de Blas, T. Rodriguez-Blas, *Inorg. Chem.* **2002**, *41*, 5336–5349.

Received: December 12, 2006
Published Online: April 16, 2007

